ASSESSMENT OF THE PROPERTIES OF HAp MICROPOWDERS AFTER ION EXCHANGE PROCESS IN SILVER NITRATE SOLUTION

Marta Głuszek[1] , Zuzanna Świrska[1] , Witold Kaczorowski[1]* , Bartłomiej Januszewicz[1] , Maciej Wrotniak[2]

[1] Institute of Materials Science and Engineering, Lodz University of Technology, Stefanowskiego 1/15, 90-924 Lodz, Poland
[2] Clinical Department of Orthopedic-Traumatic, Oncological and Reconstructive Surgery, St. Barbara Specialized Regional Hospital No. 5, Sosnowiec, Plac Medyków 1, 41-200 Sosnowiec, Poland
*e-mail: witold.kaczorowski@p.lodz.pl

Abstract

Bioceramic materials, such as hydroxyapatite (HAp), are characterized by high biocompatibility in the presence of tissues and body fluids without causing toxic or allergic reactions. Hydroxyapatite, due to its similarity to structures found in bones, is used both in the form of powders, e.g. as additives to bone cements, and implants coatings. However, this material is not characterized by antimicrobial properties, therefore attempts are made to improve its properties by introducing additional elements into the hydroxyapatite structure. Thanks to HAp's high ion-exchange ability, silver can be introduced into its structure. The calcium ions present in the HAp structure can be easily replaced by silver ions to create a material endowed with high biocompatibility and antibacterial properties. The presented study is based on the analysis of the morphology of the modified powders via scanning electron microscopy (SEM), their chemical composition via X-ray energy dispersive spectroscopy (EDS) and chemical structure via X-ray diffraction (XRD) and Raman spectroscopy. The powders obtained through the ion exchange were mixtures of silver phosphates Ag_3PO_4 and HAp. The highest silver content was found in the sample modified with a 1M concentration of $AgNO_3$ in the aqueous solution. It was also determined that the annealing of the obtained powders under vacuum at 800°C resulted in the formation of metallic silver and a change in the structure of HAp to β-TCP.

Keywords: hydroxyapatite, ion exchange, silver nitrate (V), annealing, XRD, Raman spectroscopy

Introduction

Hydroxyapatite $Ca_{10}(PO_4)_6(OH)_2$ belongs to the group of apatite minerals with a Ca/P molar ratio of 1.667. It has a hexagonal structure tightly packed with atoms, therefore this compound has a rather high density - 3.16 g/cm³ [1,2]. Hydroxyapatite is a biologically active material whose chemical and phase composition is similar to that of human bone. The biggest advantage of hydroxyapatite is its porosity which gives the possibility of bone tissue ingrowth [3,4]. In addition, the mere presence of calcium and phosphorus ions at the interface between the ceramic and the bone tissue enables faster bonding between the bone and the implant [5-7]. HAp dissolves relatively well in acids and poorly in water. It is characterized by a high ion exchange capacity [8-10]. One way to modify hydroxyapatite is to incorporate silver into its structure [11-13]. W. Chen et al. [14] and M. Rai et al. [15] showed that HAp is an optimal material for introducing silver ions. The Ca^{2+} ions present in the HAp structure can be easily replaced by Ag^+ ions, creating a material with high biocompatibility and antibacterial properties. The antibacterial properties of silver have been used in many fields of medicine for years, which is evidenced by the wide range of preparations available on the market [16]. Since ancient times silver has been used in the treatment of extensive wounds and burns [17,18]. Silver in small amounts has low toxicity to human cells, high thermal stability, and low volatility with prolonged action, indicating biofilm inhibitory properties [19,20]. It is worth noting that some implant rejections may result from the disconnection of the implant surface and bone tissue, due to inflammation associated with local infection. To reduce the risk of peri-implant infection, antibiotic prophylaxis is commonly used [21-23]. Nowadays, there is more and more research on the use of materials endowed with local antibacterial activity. Among them, silver-doped coatings (DLC - diamond-like carbon, HAp) seem to be promising [24-28]. As shown in the literature, the introduction of silver into HAp coatings can be carried out in various ways [29,30]. One of the possibilities is the application of powders containing both hydroxyapatite and silver in the coating manufacturing processes [31,32]. The present work addresses precisely this issue. It describes an ion exchange process using hydroxyapatite powder and silver nitrate (V) solutions. The efficiency of such a process is influenced by the following factors: pH, temperature, and the solution concentration where the reaction takes place. pH parameter determines the degree of dissociation of functional groups, which has a bearing on the dynamics and efficiency of the process. On the other hand, increasing the temperature of the process accelerates the ion exchange reaction. This happens due to the internal structure loosening of the ionite particle so that the transport of ions into the structure is much easier. The ion exchange process is also affected by the structure of the ionite particles, the type of ions exchanged, the type and number of functional groups in the ionite, and the efficiency of ionite regeneration [33,34]. The ion exchange processes carried out in this work, using hydroxyapatite powder and different concentrations of silver nitrate (V) solution, enabled the formation of a silver-containing compound (Ag_3PO_4) from which metallic silver can be obtained by annealing [35-37]. Therefore, the paper also includes the results from a trial annealing process of a selected powder at 800°C.

Materials and Methods

Hydroxyapatite ($Ca_{10}(PO_4)_6(OH)_2$) powder from MEDI-COAT used for the plasma spraying of coatings and the silver nitrate (V) $AgNO_3$ solution from P.P.H. "STANLAB" Sp. J. were used for the ion exchange process. In the first step, $AgNO_3$ solutions were prepared at concentrations: 1M and 4M. An appropriately determined mass of silver nitrate $AgNO_3$ was dissolved in deionized water at 50°C using a magnetic stirrer. An equal amount of hydroxyapatite powder was then added to the solutions. The ion exchange was carried out for a 7 pH solution. To obtain the intended pH of the suspensions, 65% HNO_3 was gradually added. The obtained suspensions were stirred at a constant temperature of 50°C for 30 min. Then, all the suspensions were subjected to decantation three times. Finally, the obtained products were dried for 48 h at room temperature and then for 24 h in a vacuum dryer at 100°C. The obtained samples were designated as Ag-HAp-1M and Ag-HAp-4M, respectively. The sample with the highest concentration of silver was subjected to annealing in a vacuum oven (at about 10^{-3} Pa) at 800°C for 1 hour.

Morphology studies of the modified HAp and Ag-HAp powders were performed using a JSM-6610LV Scanning Electron Microscope (JEOL, USA) equipped with an EDS chemical composition analysis attachment (X-Max 80 EDS; Oxford Instruments, UK). Surface topography images of the samples were taken using secondary electrons. Observations were made under high vacuum, with accelerating voltage from 10 to 15 kV. The phase composition analysis was carried out using an EMPYREAN X-ray diffractometer from PANalytical, operating in Theta-Theta geometry at 40 kV and 45 mA current, using Co lamp X-rays with wavelength λ = 1.7902 Å. To confirm the changes in the chemical structure of the powders, the Raman Spectroscopy technique was applied, using an inVia Confocal Raman spectrometer from Renishaw (Gloucestershire, UK) using a 532 nm laser.

Results and Discussion

The SEM images show the morphology of the HAp powders before and after the modification processes. FIG. 1a shows the characteristic structure of the HAp powders. As can be seen, there are agglomerates of smaller particles with irregular shapes (FIG. 1a). After the ion exchange processes their morphology changes, which is indicated by more regular particle shapes (FIG. 1b,c). All the samples show a rather large scatter of microparticle sizes from about 20 to 130 μm. None of the modifications applied significantly changed their sizes.

In order to check the effectiveness of the performed processes, the samples were subjected to the EDS analysis to determine their basic chemical composition (FIG. 2). As can be seen, the Ag-HAp-1M sample had the highest silver content (18.52% on an atomic scale). Usege of the higher concentration of $AgNO_3$ in the solutions inhibits the ion exchange process, and the powders obtained in this way had about 15.05% silver in their atomic composition.
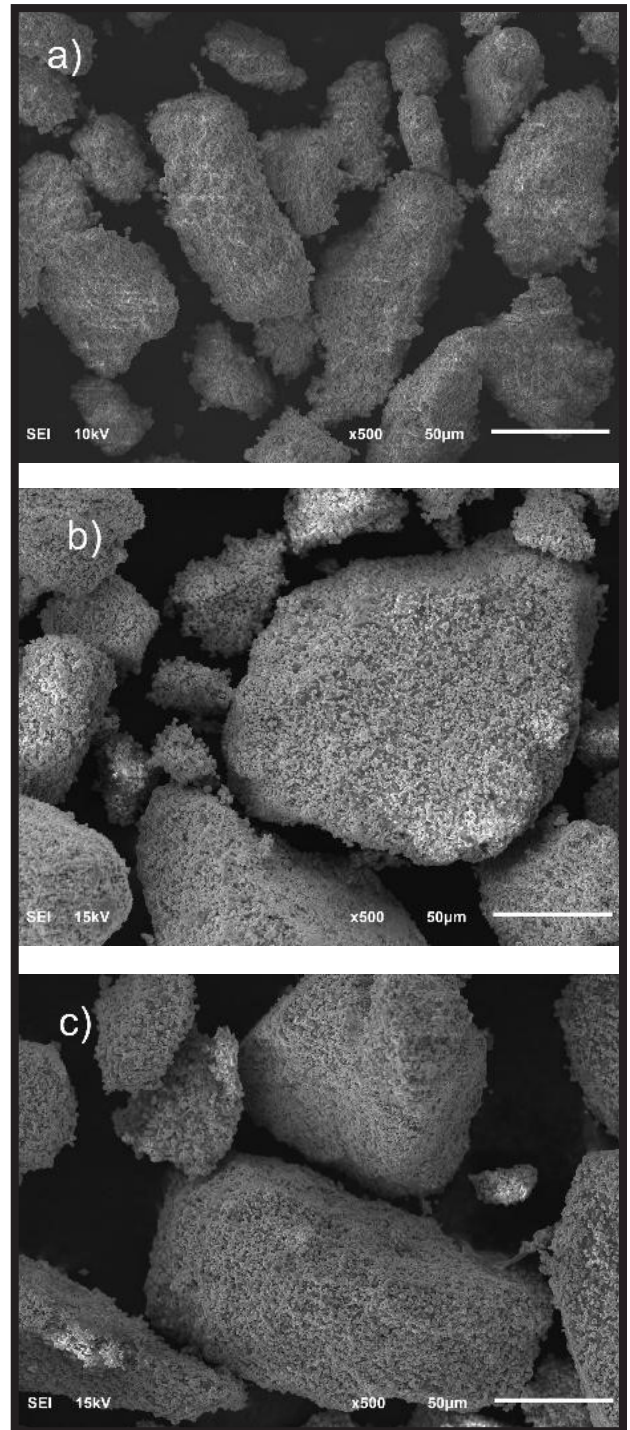
FIG. 1. SEM pictures of surface morphology: a) HAp, b) Ag-HAp-1M, c) Ag-HAp-4M.
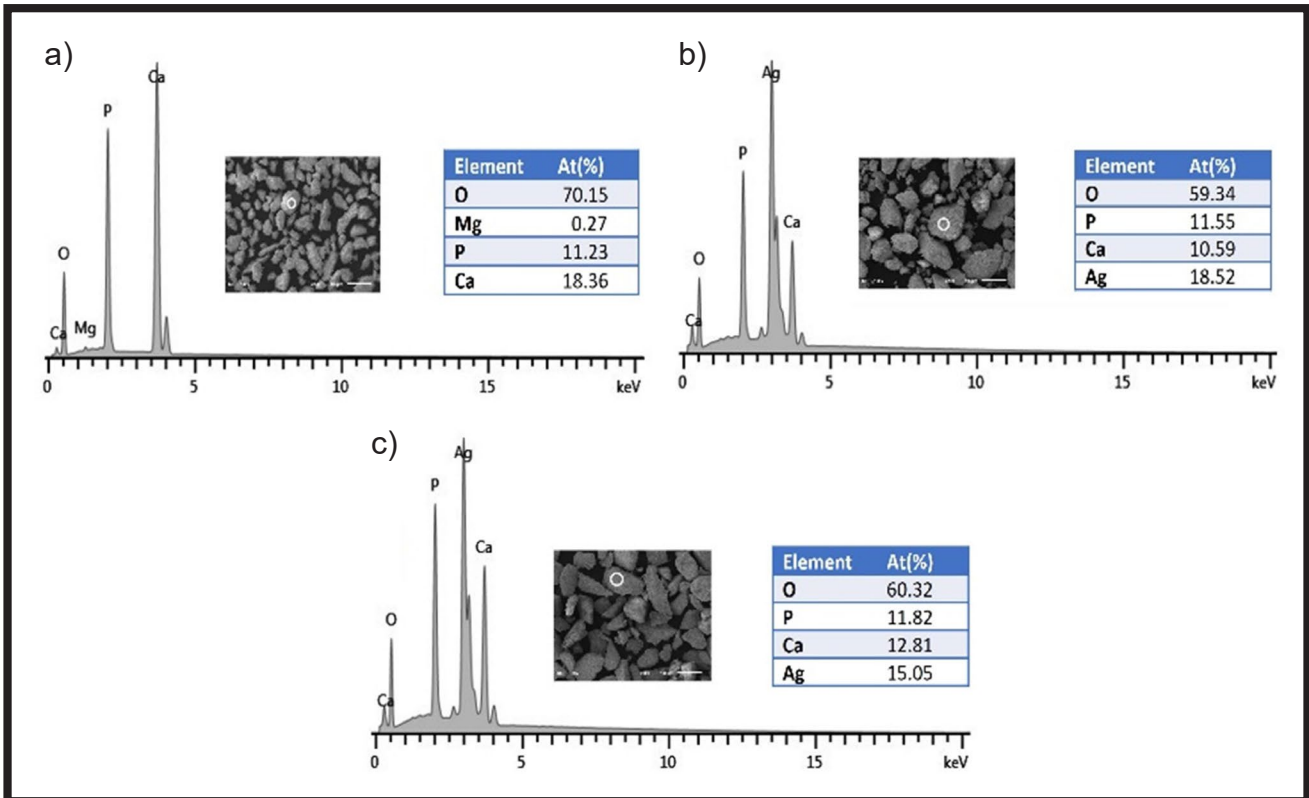
FIG. 2. EDS analysis of the micropowders: a) HAP, b) Ag-HAp-1M, c) Ag-HAp-4M.
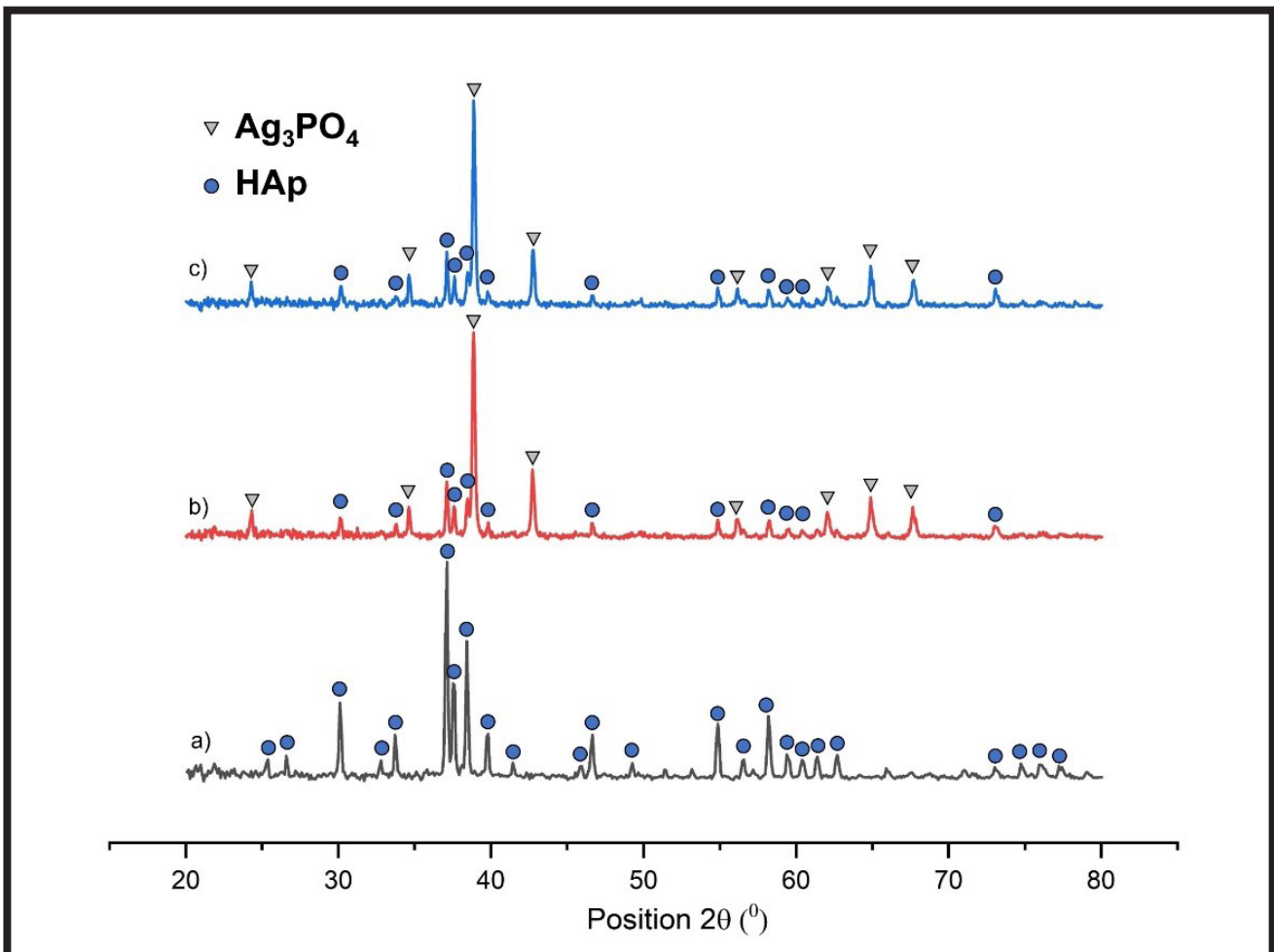
FIG. 3. X-ray patterns of analyzed micropowders: a) HAp, b) Ag-HAp-1M, c) Ag-HAp-4M.

Further analysis of the ion exchange process was made by XRD technique and Raman Spectroscopy. FIG. 3 shows the diffractograms obtained for the powders before and after modification. This study did not reveal any other crystalline phases in the powders except for HAp (according to the standard number 00-009-0432) and Ag₃PO₄ (according to the standard number 04-009-5227). Their simultaneous presence is evidence that the selected conditions enabled only a partial exchange of Ca²⁺ ions to Ag⁺ in HAp powders. For HAp powders, distinct diffraction peaks which corresponded to specific crystallographic planes of the hexagonal cell were found at the following angular positions: 25.39 (200); 26.65 (111); 30.14 (002); 32.78 (102); 33.76 (210); 37.07 (211); 37.56 (112); 38.39 (300); 39.75 (202); 41.44 (301); 45.85 (212); 46.58 (310); 49.22 (311); 54.82 (222); 56.49 (312); 58.14 (213); 59.37 (321); 60.33 (410); 61.32 (402); 62.59 (004); 73.04 (214); 74.72 (502); 76.05 (323.304); 77.25 (511). After the modification processes in the powders, in addition to the selected HAp diffraction peaks, the peaks characteristic for the Ag₃PO₄ cubic structure were observed at the following angular positions: 24.30 (110); 34.63 (200); 38.88 (210); 42.76 (211); 56.15 (310); 62.07 (222); 64.91 (320); 67.68 (321). Additionally, the analysis based on the Rietveld method showed that in Ag-HAp-1M powders the Ag₃PO₄ phase accounted for 43.5% while in Ag-HAp-4M powders only 35.2%. The trend of these changes is also visible in the intensity of the characteristic peaks on the diffractograms shown in FIG. 3.

FIG. 4 presents the Raman spectra of the studied powders. The spectrum of the unmodified hydroxyapatite (4a) according to the literature [38-41] shows the most intense peak characteristic of symmetric stretching vibrations around 963 cm⁻¹ (character 1) between P-O-P within the (PO₄)³⁻ tetrahedral.

Further, peaks at about 1072, 1046 and 1029 cm⁻¹ respectively, correspond to the symmetric streching vibrations. Modes at about 593 and 581 cm⁻¹ are associated with (4) O-P-O vibrations and at about 431 cm⁻¹ with (2) O-P-O vibrations. After modification in the aqueous AgNO₃ solution, the most prominent peak on the Raman spectrum is at the position of about 909 cm⁻¹ originating from the stretching symmetric vibrations of (1) PO₄³⁻ evidently indicating the formation of Ag₃PO₄ [42,43]. In addition, typical modes from the unmodified HAp powder (especially at 963 cm⁻¹) are visible to a lesser extent. For powders modified in AgNO₃ solution, the peaks at 909 cm⁻¹ and 963 cm⁻¹ change their intensities according to the content of silver atoms in the samples. The lowest intensity of the peak characteristic for the pure HAp powder (at 963 cm⁻¹), and at the same time the highest intensity of the peak characteristic for the Ag₃PO₄ structures (at 909 cm⁻¹) are typical for the Ag-HAp-1M powders with the highest silver content and the highest content of Ag₃PO₄ phase.

The mixture of silver phosphate and hydroxyapatite obtained in the ion exchange process with the highest silver content was subjected to a one-hour annealing process in a vacuum oven at 800°C in order to confirm the possibility of changing the structure of the modified powders to the one with silver in a metallic form and not in the Ag₃PO₄ compound. After this process, the powders were re-examined using the techniques presented earlier. FIG. 5 presents the SEM image of the powder modified in this way along with EDS analysis, while FIG. 6 shows the characteristic XRD and Raman spectroscopy spectra. As can be seen in FIG. 5, the morphology of the powders changed. After the annealing process, the micropowders were composed of spherically shaped, sintered particles.
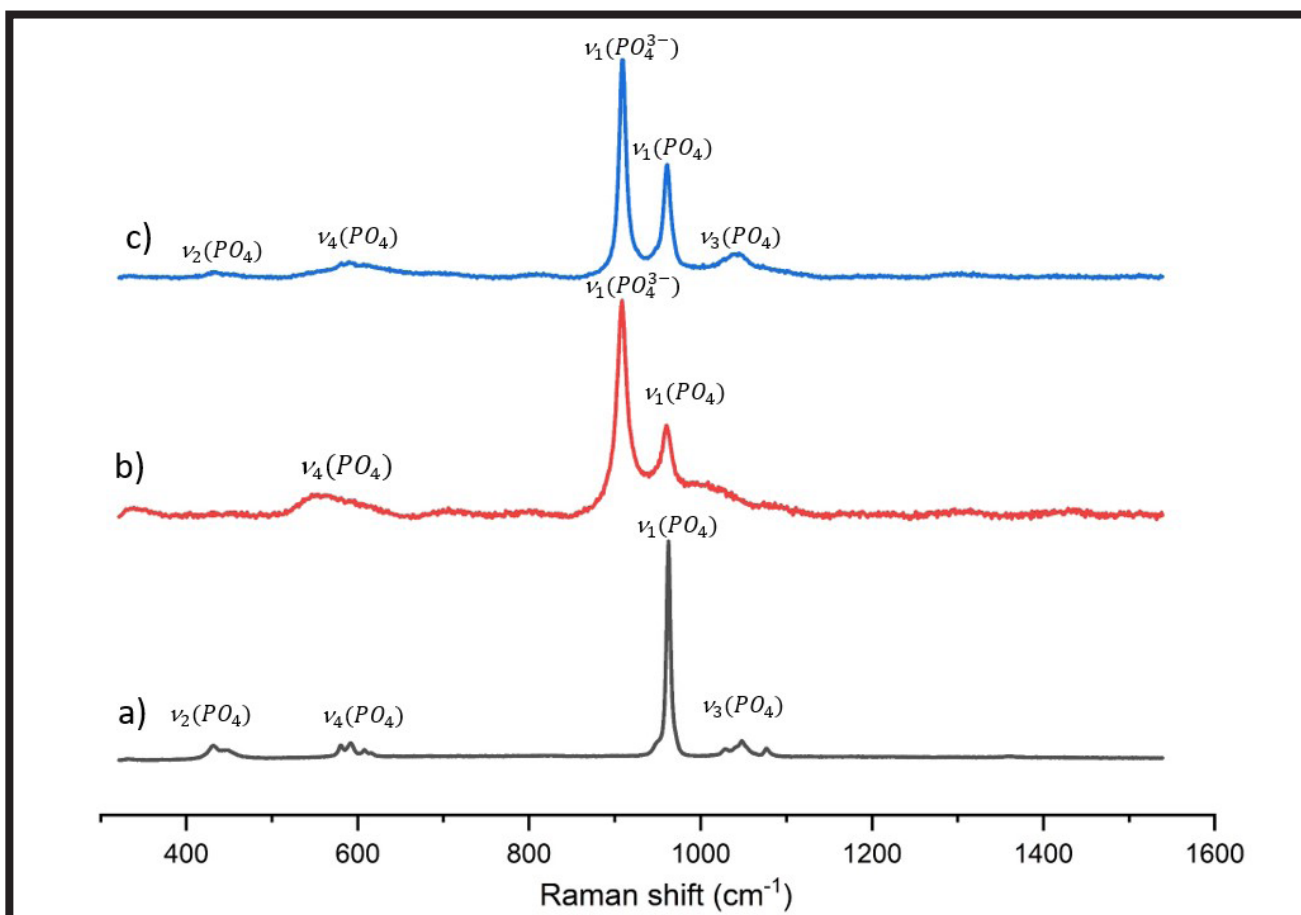
FIG. 4. Raman spectra of micropowders: a) HAp, b) Ag-HAp-1M, c) Ag-HAp-4M.
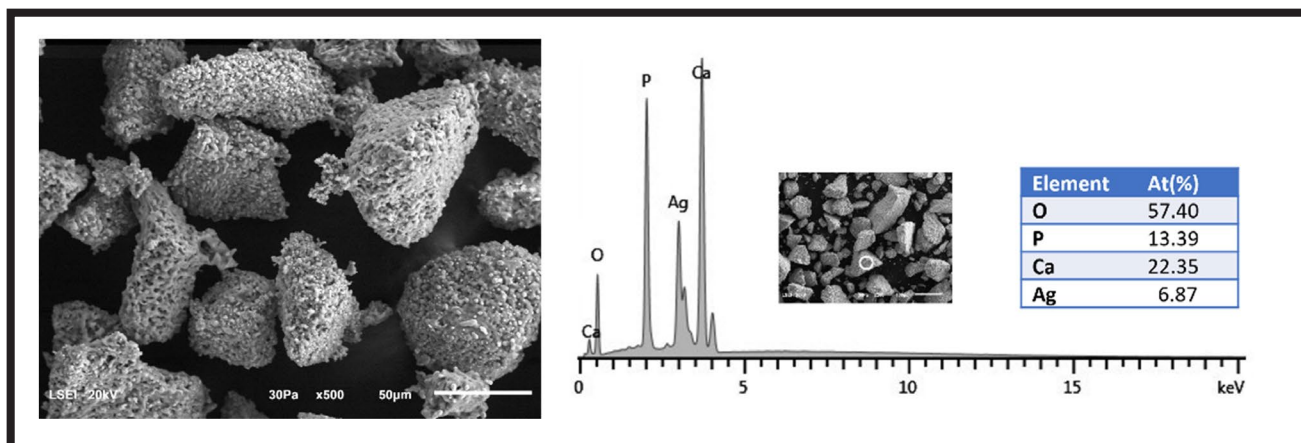
FIG. 5. Surface morphology and EDS analysis of heated micropowders Ag-HAp-1M.

Element	At(%)
O	57.40
P	13.39
Ca	22.35
Ag	6.87
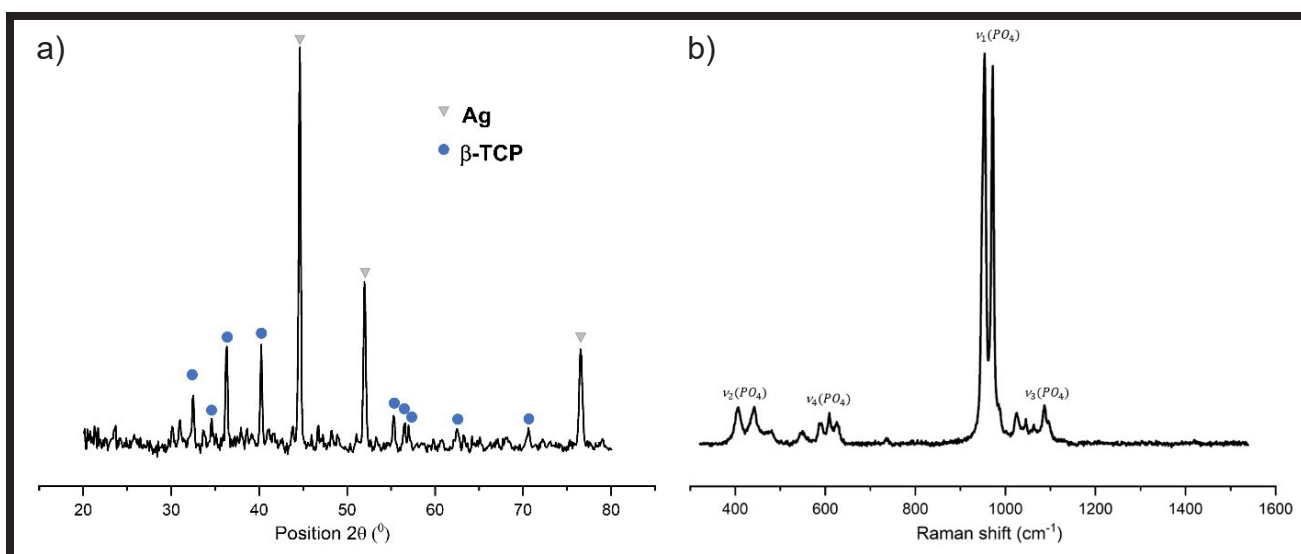
FIG. 6. X-ray pattern of phase composition (a) and Raman spectrum (b) of Ag-HAp-1M powder.

From the EDS studies, it can be seen that the silver content of these powders was lower than the Ag-HAp-1M powders, which may be due to the temperature and pressure of the processing. After annealing, the characteristic peaks of the silver cubic structure were observed in the studied powders (FIG. 6a) at the following angular positions: 44.57 (111); 51.95 (200); 76.53 (220) and rhombohedral -TCP at the following angular positions: 32.36 (214); 34.57 (300); 36.19 (0210); 40.13 (220); 55.13 (4010); 56.33 (238); 56.85 (416); 62.35 (2020); 70.38 (517). The Raman spectrum in FIG. 6b shows the change of the HAp powder in –TCP, as evidenced by the $\nu_1(PO_4)$ modes occurring at about 949 cm^{-1} and 971 cm^{-1} [43-45]. The other peaks were attributed to the $\nu_2(PO_4)$ vibrations occurring at about 406, 442, 481 cm^{-1}, $\nu_3(PO_4)$ at about 1016, 1048 cm^{-1}, and $\nu_4(PO_4)$ at about 546, 598, 609, and 628 cm^{-1}.

Conclusions

The ion exchange process led to the incorporation of silver ions into the hydroxyapatite structure. This confirmed the effectiveness of the procedure used to obtain the powders as Ag_3PO_4/HAp mixtures. The morphology of the HAp powders changes significantly as a result of silver doping. The phase composition analysis revealed the presence of characteristic peaks corresponding to HAp and the newly formed silver phosphate phase Ag_3PO_4.

The sample modified with 1M AgNO$_3$ in an aqueous solution had the highest silver content. Additionally, the chemical and phase composition of the produced powders can be modified by thermal treatment. The use of vacuum annealing at 800°C resulted in the formation of metallic silver and the change in the structure of HAp to β-TCP. However, further studies and analyses are necessary to precisely develop process parameters for the modification of HAp powders with silver ions, as well as their thermal treatment.

ORCID iDs
M. Głuszek: https://orcid.org/0000-0002-6096-988X
Z. Świrska: https://orcid.org/0000-0001-8175-2762
W. Kaczorowski: https://orcid.org/0000-0001-7193-0473
B. Januszewicz: https://orcid.org/0000-0001-8735-0975
M. Wrotniak: https://orcid.org/0000-0002-4329-8623

References

[1] Ślósarczyk A., Potoczek M., Paszkiewicz Z., Zima A., et al.: Characteristics and biological evaluation of high-porosyapatite bioceramics. Ceramic Materials 62(2) (2010) 224-229.

[2] Sobczak-Kupiec A., Wzorek Z.: Właściwości fizykochemiczne ortofosforanów wapnia istotnych dla medycyny - TCP i HAp. Chemia. Czasopismo techniczne 107 (2010) 309-322.

[3] Kluess D., Bergschmidt P. Mittelmeier, W.: Ceramics for joint Replacement. Joint Replacement Technology, (2014) 152-166.

[4] Gremillard L., Chevalier J.: New Trends in Ceramics for Orthopedics. Encyclopedia of Materials: Technical Ceramics and Glasses 3 (2021) 493-500.

[5] Arcos D., Vallet-Regi M.: Substituted hydroxyapatite coatings of bone implants. Journal of Materials Chemistry B, 8(9) (2020) 1781-1800.

[6] Wang X., Yu Y., Ji L., et. al.: Calcium phosphate-based materials regulate osteoclast-mediated osseointegration. Bioactive Materials 6(12) (2021) 4517-4530.

[7] Święcicki Z.: Bioceramika dla ortopedii. Instytut Pods. Problemy Techniki PAN, Wyd. Spółdzielcze Sp. z o.o., Warsaw, 1992.

[8] Rujitanapanich S., Kumpapan P., Wanjanoi P.: Synthesis of Hydroxyapatite from Oyster Shell via Precipitation. Energy Procedia 56 (2014) 112-117.

[9] Szcześ A., Hołysz L., Chibowski E.: Synthesis of hydroxyapatite for biomedical applications, Advances in Colloid and Interface Science 249 (2017) 321-330.

[10] Gaoyu Ch., Xiaoyan Z., Chong W., Junfeng H., et al.: A postsynthetic ion exchange method for tunable doping of hydroxyapatite nanocrystals. RSC Advances, 7(89) (2017) 56537-56542.

[11] Hou J., Liu Y., Han Z., et al.: Silver-hydroxyapatite nanocomposites prepared by three sequential reaction steps in one pot and their bioactivities in vitro. Materials Science and Engineering C 120 (2021) 111655.

[12] Dubnika A., Loca D., Rudovica V., et al.: Functionalized silver doped hydroxyapatite scaffolds for controlled simultaneous silver ion and drug delivery. Ceramics International 47 (2017) 3698-3705.

[13] Šupová M.: Substituted hydroxyapatites for biomedical applications: A review, Ceramics International 41(8) (2015) 9203-9231.

[14] Chen W., Liu Y., Courtney H.S., Betteng M., Agrawal C.M., et al.: In vitro anti-bacterial and biological properties of magnetron co--sputtered silver-containing hydroxyapatite coating. Biomaterials 27(32) (2006) 5512-5517.

[15] Rai M., Yadav A., Gade A., et al.: Silver nanoparticles as a new generation of antimicrobials. Biotechnology Advances 27(1) (2009) 76-83.

[16] Lysakowska M., Denys P.: Antimicrobial uses of silver. Antimicrobial uses of silver. Ortop 4 Quarter, (2009) 408-417.

[17] Klasen H.J.: A historical review of the use of silver in the treatment of burns. II. Renewed interest for silver, Burns 26(2) (2000) 131-138.

[18] Moiemen N.S., Shale E., Drysdale K.J., et al.: Acticoat dressings and major burns: Systemic silver absorption. Burns 37 (2011) 27-35.

[19] Bugla-Płoskońska G., Oleszkiewicz A.: Biological activity of silver and its application in medicine. Cosmos – Problems of Biological Sciences 56(1-2) (2007) 115-122.

[20] Yang J.Y., Huang C.Y., Chuang S.S., et al.: Case report: A clinical experience of treating exfoliative wounds using nanocrystalline silver-containing dressings (Acticoat). Burns 33 (2007) 793-797.

[21] Lansdown A.B.G.: Silver. I: its antibacterial properties and mechanism of action. Journal of Wound Care 11(4) (2013) 125.

[22] Petica A., Gavriliu S., Lungua M., et al.: Colloidal silver solutions with antimicrobial properties. Materials Science and Engineering: B 152 (2008) 22-27.

[23] Sandukas S., Yamamoto A., Rabiei A.: Osteoblast adhesion to functionally graded hydroxyapatite coatings doped with silver. J. Biomed. Mater. Res. 97(4) (2011) 490-497.

[24] Ratha I., Datta P., Balla V. K., et al.: Effect of doping in hydroxyapatite as coatings material on biomedical implants by plasma spraying method; A rewiew. Ceramics Internationals 47(4) (2021) 4426-4445.

[25] Ressler A., Žužić A., et al.: Ionic substituted hydroxyapatite for bone regeneration applications: A review. Open Ceramics 6 (2021) 100122.

[26] Lei Song, Yan-Feng, Xiao Lu Gan, et al.: The effect of antibacterial ingredients and coating microstructure on the antibacterial properties of plasma sprayed hydroxyapatite coatings. Surface and Coatings Technology 206(11-12) (2012) 2986-2990.

[27] Kolmas J., Piotrowska U., Kuras M., et al.: Effect of carbonate substitution on physicochemical and biological properties of silver containing hydroxyapatites. Materials Science and Engineering: C 74(1) (2017) 124-130.

[28] Cazalini E.M., Miyakawa W., Teodoro, G.R., et al.: Antimicrobial and anti-biofilm properties of polypropylene meshes coated with metal-containing DLC thin films. Journal of materials science. Materials in medicine 28(6) (2017) 97.

[29] Chen W., Oh S., Ong A.P., Oh N., et al.: Antibacterial and osteogenic properties of silver-containing hydroxyapatite coatings produced using a sol gel process. The Japanese Society for Biomaterials, and The Australian Society for Biomaterials and the Korean Society for Biomaterials 82(4) (2007) 899-906.

[30] Yajing Y., Xuejiao Z., Yong H., et al.: Antibacterial and bioactivity of silver substituted hydroxyapatite/TiO$_2$ nanotube composite coatings on titanium. Applied Surface Science 314(30) (2014) 348-357.

[31] Bensalema A., Kaan Kucukosman O., Raszkiewicz J.: Synthesis, characterization, bactericidal activity, and mechanical properties of hydroxyapatite nano powders impregnated with silver and zinc oxide nanoparticles (Ag-ZnO-Hap). Ceramics International 47(15) (2021) 21319-21324.

[32] Wahhab Abdulsada F., Ali Sabea Hammood: Characterization of corrosion and antibacterial resistance of hydroxyapatite/silver nano particles powder on 2507 duplex stainless steel. Materialstoday proceedings 42(5) (2021) 2301-2307.

[33] Zagorodni A.A.: Physico-chemical Description of Ion Exchange Processes. Ion Exchange Materials, Properties and Applications, Elsevier (2007) 169-198.

[34] De Trizio L., Manna L.: Forging Colloidal Nanostructures via Cation Exchange Reactions. 116(18) (2016) 1085210887.

[35] M.M.J. van Rijt, S.W. Nooteboom, et al.: Stability-limited ion-exchange of calcium with zinc in biomimetic hydroxyapatite. Materials & Design 207 (2021) 109846.

[36] Riaz M., Zia R., Ijaz A.: Synthesis of monophasic Ag doped hydroxyapatite and evaluation of antibacterial activity. Materials Science and Engineering: C 90(1) (2018) 308-313.

[37] Hong X., Wu X., Zhang Q., Xiao M.: Hydroxyapatite supported Ag$_3$PO$_4$ nanoparticles with higher visible light photocatalytic activity. Applied Surface Science 258(10) (2012) 4801-4805.

[38] Chai B., Jing L., Qian X.: Reduced Graphene Oxide Grafted Ag$_3$PO$_4$ Composites with Efficient Photocatalytic Activity under Visible-Light Irradiation, Ind. Eng. Chem. Res. 53 (2014) 8744-8752.

[39] Klinkaewnarong J., Swatsitang E., Masingboon Ch., Seraphin S., Maensiri S.: Synthesis and characterization of nanocrystalline HAp powders prepared by using aloe vera plant extracted solution. Current Applied Physics 10 (2010) 521-525.

[40] Silva C.C., Sombra A.S.B.: Raman spectroscopy measurements of hydroxyapatite obtained by mechanical alloying. Journal of Physics and Chemistry of Solids 65 (2004) 1031-1033.

[41] Koutsopoulos S.: Synthesis and characterization of hydroxyapatite crystals: A review study on the analytical methods. Journal of Biomedical Materials Research 62 (2002) 600-612.

[42] Hua T., Yanhui F., Shufang Ch., Siyu X., Guogang T.: Construction of Ag$_3$PO$_4$/Ag$_2$MoO$_4$ Z-scheme heterogeneous photocatalyst for the remediation of organic pollutants. Chinese Journal of Catalysis 38 (2017) 337-347.

[43] Penel G., Cau E., Delfosse C., Rey Ch., Hardouin P., Jeanfils J., et al.: Raman Microspectrometry Studies of Calcified Tissues and Related Biomaterials. Raman Studies of Calcium Phosphate Biomaterials. Dent. Med. Probl. 40(1) (2003) 37-43.

[44] Carrodeguas R.G., De Aza S.: α-Tricalcium phosphate: Synthesis, properties and biomedical applications. Acta Biomaterialia 7 (2011) 3536-3546.

[45] Aruna S.T., Kulkarni S., Chakraborty M., et al.: A comparative study on the synthesis and properties of suspension and solution precursor plasma sprayed hydroxyapatite coatings. Ceramics International 43 (2017) 9715-9722.